Chemistry and technology of inorganic materials

Химия и технология неорганических материалов

RESEARCH ARTICLE

Synthesis of complex oxides Eu_2O_3–Gd_2O_3–$Zr(Hf)O_2$ using microwave radiation and study of their properties

Nikolay V. Grechishnikov ✉, **Elena E. Nikishina**

MIREA – Russian Technological University (Lomonosov Institute of Fine Chemical Technologies), Moscow, 119454 Russia

✉ *Corresponding author, e-mail: nklgrchshnkv@yandex.ru*

Abstract

Objectives. The authors synthesize complex oxide phases of the composition $Eu_{2-x}Gd_xZr_2O_7$ and $Eu_{2-x}Gd_xHf_2O_7$ at $x = 0.5, 1.0, 1.5$ under microwave heating conditions and investigate their phase composition, particle size distribution, and specific surface with the purpose of obtaining bulk ceramic materials on their basis and study their behavior when heated to 1473 K.

Methods. Using X-ray phase analysis, the phase composition of samples subjected to heat treatment at temperatures of 1473 and 1773 K was studied, and the cell parameters were calculated. The particle size of the obtained powders was analyzed by laser diffraction on a Fritsch Analysette 22 device. The specific surface area was studied by the Brunauer–Emmett–Teller method on a TriStar 3000 analyzer. Bulk ceramic materials were obtained by cold pressing with subsequent sintering at 1773 K. The coefficient of thermal expansion (CTE) of ceramic samples was studied on a Netzsch DIL 402C dilatometer in a temperature range of 300–1473 K.

Results. At a temperature of 1473 K, all synthesized samples were observed to form a fluorite structure; at a temperature of 1773 K, samples with the composition $Eu_{2-x}Gd_xHf_2O_7$ had an ordered pyrochlore structure. With an increase in the gadolinium content in the samples, a decrease in both the unit cell parameter and the CTE was observed. The particle size of almost all samples did not exceed 100 μm; the specific surface area did not exceed 1 m²/g.

Conclusions. For the first time, compounds with the composition $Eu_{2-x}Gd_xZr_2O_7$ and $Eu_{2-x}Gd_xHf_2O_7$ were obtained using microwave processing at $x = 0.5, 1.0, 1.5$. As well as determining the dependence of the phase composition on the heat treatment temperature after microwave exposure, the dependence of the change in the unit cell parameters on the gadolinium content in the sample was studied, the particle size distribution was investigated. The CTEs of bulk ceramic samples obtained by cold pressing were additionally studied. The obtained data can be used in the development of thermal barrier coatings and technical ceramics used at high temperatures (up to 1473 K).

НАУЧНАЯ СТАТЬЯ

Синтез сложных оксидов Eu_2O_3–Gd_2O_3–$Zr(Hf)O_2$ с применением микроволнового излучения и исследование их свойств

Н.В. Гречишников ✉, **Е.Е. Никишина**

МИРЭА – Российский технологический университет (Институт тонких химических технологий им. М.В. Ломоносова), Москва, 119454 Россия

✉ *Автор для переписки, e-mail: nklgrchshnkv@yandex.ru*

Аннотация

Цели. Синтезировать сложнооксидные фазы состава $Eu_{2-x}Gd_xZr_2O_7$ и $Eu_{2-x}Gd_xHf_2O_7$ при x = 0.5, 1.0, 1.5 в условиях микроволнового нагрева, исследовать их фазовый состав, распределение частиц по размеру и удельную поверхность, получить на их основе объемные керамические материалы и изучить их поведение при нагревании до 1473 K.

Методы. С помощью рентгенофазового анализа проведено исследование фазового состава образцов, прошедших термическую обработку при разных температурах 1473 и 1773 K, а также рассчитаны параметры ячейки. Анализ размера частиц полученных порошков проводили методом лазерной дифракции на приборе Fritsch Analysette 22. Площадь удельной поверхности исследовали методом Брунауэра–Эммета–Теллера на анализаторе TriStar 3000. Объемные керамические материалы получали холодным прессованием с последующим спеканием при 1773 K. Исследование коэффициента линейного термического расширения (КЛТР) керамических образцов проводили на дилатометре Netzsch DIL 402C в интервале температур 300–1473 K.

Результаты. Установлено, что при температуре 1473 K у всех синтезированных образцов образуется структура флюорита, а при температуре 1773 K образцы с составом $Eu_{2-x}Gd_xHf_2O_7$ имеют упорядоченную структуру пирохлора. При увеличении содержания гадолиния в образцах наблюдается уменьшение как параметра элементарной ячейки, так и КЛТР. Размер частиц практически всех образцов не превышает 100 мкм, а площадь удельной поверхности не превышает 1 м²/г.

Выводы. Впервые с применением микроволновой обработки получены соединения с составом $Eu_{2-x}Gd_xZr_2O_7$ и $Eu_{2-x}Gd_xHf_2O_7$ при x = 0.5, 1.0, 1.5, изучена зависимость фазового состава от температуры термообработки после микроволнового нагрева, изучена зависимость изменения параметров элементарной ячейки от содержания гадолиния в образце, исследовано распределение частиц по размерам, а также методом холодного прессования получены объемные керамические образцы, для которых изучен КЛТР. Полученные данные могут применяться при разработке термобарьерных покрытий и технической керамики, эксплуатируемой при высоких температурах (до 1473 K).

INTRODUCTION

In recent years, zirconates and hafnates of rare earth elements (REE) (Ln_2Zr/Hf_2O_7, where Ln = La–Lu) have been actively considered in the development of materials for parts of aggregates operating in aggressive environments and high temperatures. The most extensive area of practical application of these compounds is considered to be the creation of thermal barrier coatings, antioxidant coatings and high-temperature ceramics [1]. For such purposes, REE zirconates and hafnates with an ordered pyrochlore structure, in which the ratio of ionic radii $r(Ln^{3+})/r(Zr(Hf^{4+}))$ lies in the range 1.46–1.78 [2], are generally preferred. Such materials offer greater thermal stability, as well as thermal expansion coefficients close to those for most substrates and low thermal conductivity [3]. Zirconates and hafnates having a disordered fluorite structure also find application in the field of thermal barrier coatings and other areas of science and technology, for example, for the creation of solid electrolytes, due

to oxygen defects contained in the structure of these compounds [4].

At present, individual REE zirconates and hafnates have been quite well studied. A large number of works are devoted to the study of lanthanum zirconate and lanthanum hafnate, due to these substances offering the lowest fluorite→pyrochlore phase transition temperature (~1473 K) [2, 5], as well as europium hafnate [6], gadolinium zirconate [7]. Gadolinium zirconates and gadolinium hafnates are of particular interest due to the 1.46 ratio of the ionic radius of gadolinium to that of zirconium, which represents a boundary value for the possible formation of an ordered pyrochlore structure [2].

Due to the significant demand for REE zirconates and hafnates in various industries, the development of methods for obtaining such compounds containing two or more components while maintaining the required structure (fluorite or pyrochlore) is relevant. Works also describe the replacement of a part of REE ions by cations of another element in order to change the properties of the obtained material while preserving the ordered structure [8].

The most commonly used solid-phase method of synthesis is currently not preferred due to its high energy consumption: high sintering temperatures, long duration, since the rate is determined by the diffusion of components at the grain boundary, and preliminary preparation of initial reagents [9]. Such research is mainly focused on the development of "wet" methods for the synthesis of REE zirconates. Among such methods we can emphasize precipitation methods [10] and the sol–gel method [11]. Intermediate compounds formed as a result of the corresponding chemical reactions are transformed into REE zirconate and hafnate after thermal treatment.

In other studies, in addition to high temperatures, external influence on the reaction mixture is applied to obtain a single-phase product and increase the yield of the target phase. For example, an autoclave is used in the hydrothermal method to conduct synthesis at elevated pressures [12–14]. A simpler but no less effective method used in obtaining individual and complex oxides is microwave treatment [15, 16]. This approach provides fast and uniform heating of samples, which can be used to accelerate synthesis processes and reduce energy consumption. In some cases, the synthesis temperature can be reduced as compared with traditional methods [17]. Many studies consider microwave synthesis of compositions based on zirconium and hafnium dioxides, including in combination with sol–gel method [18–21].
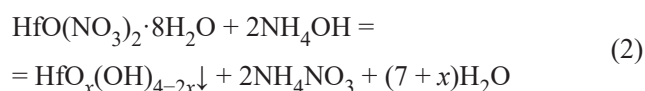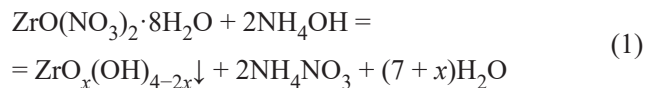
The present study is based on the preparation of Eu$_{2-x}$Gd$_x$Zr$_2$O$_7$ and Eu$_{2-x}$Gd$_x$Hf$_2$O$_7$ compounds at $x = 0.5$, 1.0, 1.5 under microwave processing conditions to study the phase composition of the obtained products, the particle size and specific surface area of the obtained powders, as well as the coefficients of thermal expansion (CTE) of ceramic materials based on them.

MATERIALS AND METHODS

For the synthesis of REE zirconates and hafnates with the composition Eu$_{2-x}$Gd$_x$Zr$_2$O$_7$ and Eu$_{2-x}$Gd$_x$Hf$_2$O$_7$ at $x = 0.5$, 1.0, 1.5, zirconium oxychloride ZrOCl$_2$·2H$_2$O (*Lankhit*, Russia), hafnium oxynitrate HfO(NO$_3$)$_2$·2H$_2$O (*Lankhit*, Russia) were used as starting reagents along with dihydrates of europium acetate Eu(CH$_3$COO)$_3$·2H$_2$O (*Lankhit*, Russia) and gadolinium acetate Gd(CH$_3$COO)$_3$·2H$_2$O (*Lankhit*, Russia). Microwave treatment of the reaction mixture was carried out in a MS-6 sample preparation system (*Volta*, Russia). Thermal treatment was carried out in a SNOL 12/16 muffle furnace (*Snol*, Russia).

The process of synthesis of complex oxides included microwave treatment of a mixture of europium and gadolinium acetates with zirconium or hafnium hydroxide followed by heat treatment. For this purpose, zirconium or hafnium hydroxide was previously prepared by reactions (1) and (2), respectively:

$$ZrO(NO_3)_2 \cdot 8H_2O + 2NH_4OH =$$
$$= ZrO_x(OH)_{4-2x}\downarrow + 2NH_4NO_3 + (7 + x)H_2O \qquad (1)$$

$$HfO(NO_3)_2 \cdot 8H_2O + 2NH_4OH =$$
$$= HfO_x(OH)_{4-2x}\downarrow + 2NH_4NO_3 + (7 + x)H_2O \qquad (2)$$

To carry out these reactions, a solution containing a threefold excess of ammonia hydrate was first heated to 333 K, then zirconium oxychloride or hafnium oxynitrate was added with stirring for 40 min. The resulting precipitates were filtered off and dispersed with ethanol. A mixture of europium and gadolinium acetate containing a stoichiometric amount of REEs was added to the resulting suspensions to form a compound of the composition Eu$_{2-x}$Gd$_x$Zr$_2$O$_7$, Eu$_{2-x}$Gd$_x$Hf$_2$O$_7$. Next, the obtained reaction mixtures were subjected to microwave treatment with a power of 600 W and a frequency of 2.45 GHz, which lasted 15 min for the Eu$_{2-x}$Gd$_x$Zr$_2$O$_7$ compound line and 18 min for the Eu$_{2-x}$Gd$_x$Hf$_2$O$_7$ compound line. The influence of microwave treatment on the phase composition was considered in [22] on the example of europium zirconate. Heat treatment carried out on the obtained powders at different temperatures did not result in the formation of speck. Table 1 presents the synthesis conditions of these samples.

Table 1. Conditions for the synthesis of complex oxide phases $Eu_{2-x}Gd_xZr_2O_7$ and $Eu_{2-x}Gd_xHf_2O_7$

No.	Composition	Time of microwave processing, min	Temperature, K / Duration, h
1	$Eu_{1.5}Gd_{0.5}Zr_2O_7$	15	1473 / 6
2	$EuGdZr_2O_7$	15	
3	$Eu_{0.5}Gd_{1.5}Zr_2O_7$	15	
4	$Eu_{1.5}Gd_{0.5}Hf_2O_7$	18	
5	$EuGdHf_2O_7$	18	
6	$Eu_{0.5}Gd_{1.5}Hf_2O_7$	18	
7	$Eu_{1.5}Gd_{0.5}Zr_2O_7$	15	1773 / 1
8	$EuGdZr_2O_7$	15	
9	$Eu_{0.5}Gd_{1.5}Zr_2O_7$	15	
10	$Eu_{1.5}Gd_{0.5}Hf_2O_7$	18	
11	$EuGdHf_2O_7$	18	
12	$Eu_{0.5}Gd_{1.5}Hf_2O_7$	18	

X-ray phase analysis (XRD) of the obtained samples was performed on a D8 Advance diffractometer (*Bruker*, USA) with CuK_α-radiation (using a 0.12 mm Ni plate as a CuK_β-radiation filter, wavelength 1.5418 Å). The signal was recorded in air over a range of angles 2θ from 10° to 90° with the following parameters: step $2\theta = 0.02°$; signal acquisition time per step—0.4 s; sample rotation speed—20 rpm. Indication of the radiographs was performed using the PDF-2 rel. database 2011[1]. Processing and analysis of radiographs were performed using the HighScore Plus[2], Origin 8[3], and RTP32[4] software package.

The specific surface was investigated by the Brunauer–Emmett–Teller (BET) method on a TriStar 3000 adsorption analyzer of specific surface and porosity (*Micromeritics*, USA).

The particle size distribution was investigated using an Analysette 22 laser particle analyzer (*Fritsch*, Germany).

Bulk ceramic samples were obtained by cold pressing followed by sintering at a temperature of 1773 K for two hours. The heating rate did not exceed 180 K/h. The open porosity of all samples did not exceed 20%; the relative density of the samples was at least 92%. The dimensions of the samples were $5 \times 5 \times 26$ mm.

Thermal expansion of ceramic samples was studied using a DIL 402C dilatometer (*NETZSCH*, Germany) in the temperature range from 273–1473 K.

RESULTS AND DISCUSSION

Figure 1 depicts the diffractograms of samples *1–6*, which show peaks characteristic of the fluorite structure (111), (200), (220), and (311).

XRD showed that despite the significant duration of heat treatment (6 h), the temperature of 1473 K was sufficient only for the formation of cubic fluorite structure ($Fm\overline{3}m$) [23], the calculated parameters of the unit cell of which are presented in Table 2.

The value of the calculated unit cell parameter is characteristic of the fluorite structure. According to literature data, the parameter *a* in the pyrochlore structure lies in the range of 10.0–11.5 Å [24]. The decreased lattice parameter with an increase of gadolinium content in the obtained compound observed in these studies is explained by the smaller ionic radius of gadolinium ($r(Eu^{3+}) = 1.066$ Å (coordination number = 8); $r(Gd^{3+}) = 1.053$ Å (coordination number = 8)) than that of europium [25]. Figure 2 depicts the dependencies of the unit cell parameter *a* on the ionic radius ratio $Ln^{3+}/Zr(Hf)^{4+}$ for each composition. Taking into account the measurement error, the obtained dependence of the parameter *a* on the ratio of ionic radius $Ln^{3+}/Zr(Hf)^{4+}$ in the compound can be considered to have a linear character.

---

[1]   International center for diffraction data (ICDD), USA, icdd.com

[2]   *Malvern Pananalytical*, United Kingdom, malvernpanalytical.com

[3]   *OriginLab Corporation*, USA, originlab.com
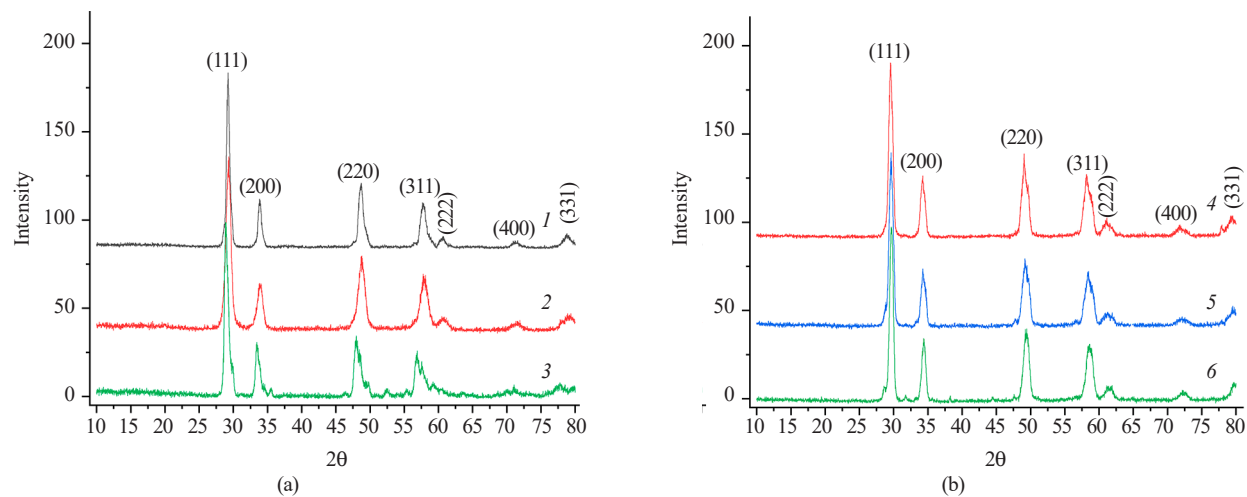
[4]   Russia, slavic.me

Fig. 1. Diffraction patterns of samples *1–3* (a) and *4–6* (b)

Table 2. Parameters of the unit cell of synthesized samples *1–6* ($T = 1473$ K)

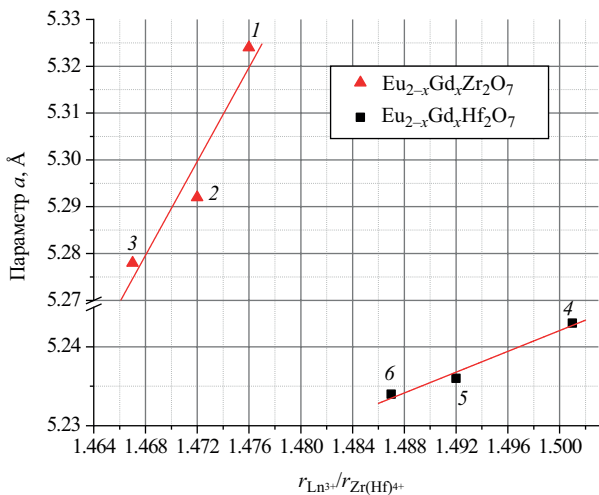| Sample	Composition	Cell parameter a, Å	Cell volume V, Å³
1	$Eu_{1.5}Gd_{0.5}Zr_2O_7$	5.324 ± 0.003	150.909 ± 0.226
2	$EuGdZr_2O_7$	5.292 ± 0.003	148.204 ± 0.222
3	$Eu_{0.5}Gd_{1.5}Zr_2O_7$	5.278 ± 0.003	147.031 ± 0.221
4	$Eu_{1.5}Gd_{0.5}Hf_2O_7$	5.243 ± 0.003	144.125 ± 0.216
5	$EuGdHf_2O_7$	5.236 ± 0.003	143.549 ± 0.215
6	$Eu_{0.5}Gd_{1.5}Hf_2O_7$	5.234 ± 0.003	143.384 ± 0.215

Fig. 2. Graph of the change in the cell parameter of the obtained samples of compounds *1–3* (markers ▲), *4–6* (markers ■)

Since the set temperature of 1473 K was sufficient only for crystallization of samples with fluorite structure, samples *7–12* were heat treated at 1773 K for 1 h.

Peaks on the diffractograms of samples *1–3* and *7–9* corresponding to the fluorite structure (Fig. 3) appear

despite the temperature of 1773 K being sufficient for the structure ordering, i.e., the transition from the fluorite structure to the pyrochlore structure [26, 27]. This may be due to the fact that even a small amount of gadolinium ions is sufficient to distort the pyrochlore lattice and thus destabilize and disorder it to the fluorite structure, whose calculated unit cell parameters are presented in Table 2.
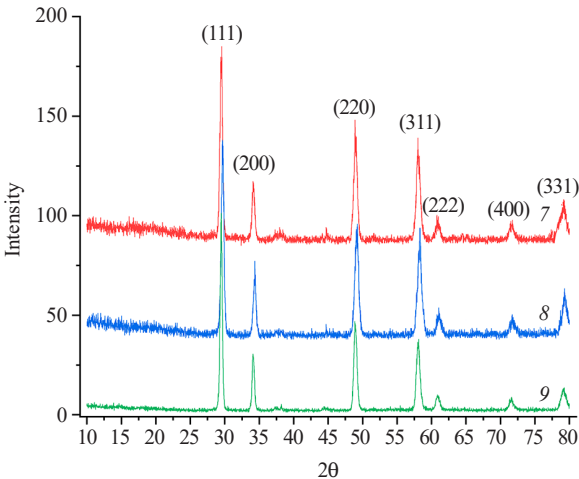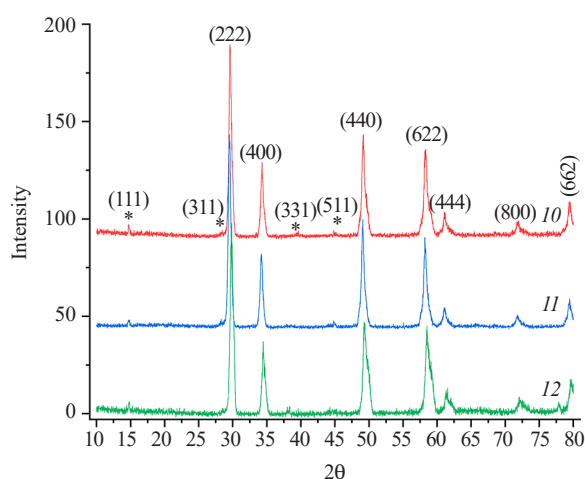

Fig. 3. X-ray diffraction pattern of samples *7–9*

Table 3. Parameters of the unit cell of synthesized samples *7–12* ($T = 1773$ K)

Sample	Composition	Cell parameter a, Å	Cell volume V, Å³
7	$Eu_{1.5}Gd_{0.5}Zr_2O_7$	5.320 ± 0.002	150.569 ± 0.226
8	$EuGdZr_2O_7$	5.300 ± 0.003	148.877 ± 0.223
9	$Eu_{0.5}Gd_{1.5}Zr_2O_7$	5.276 ± 0.003	146.8637 ± 0.220
10	$Eu_{1.5}Gd_{0.5}Hf_2O_7$	10.49 ± 0.01	1154.321 ± 1.731
11	$EuGdHf_2O_7$	10.47 ± 0.01	1147.731 ± 1.721
12	$Eu_{0.5}Gd_{1.5}Hf_2O_7$	10.45 ± 0.01	1141.166 ± 1.711

The XRD results of samples *10–12* (Fig. 4) show that all samples are crystallized with the pyrochlore structure ($Fd\bar{3}m$) [23] as indicated by the presence of additional weakly intense peaks characteristic of the pyrochlore structure: (111) at $2\theta \sim 14°$, (311) at $2\theta \sim 19°$, (331) at $2\theta \sim 34°$, (511) at $2\theta \sim 47°$. Here it is worth noting that the weak intensity of these reflexes is characteristic of this structure [26]. The calculated unit cell parameters of the obtained compounds are presented in Table 3. As indicated above, for the pyrochlore structure, the parameter a lies in the range of 10.0–11.5 Å, thus further confirming the formation of the pyrochlore structure in the compounds of the $Eu_{2-x}Gd_xHf_2O_7$ series (samples *10–12*).

Fig. 5. Graph of the change in the cell parameter of the obtained samples of compounds *7–9* (markers ▲), *10–12* (markers ■)

Fig. 4. X-ray diffraction pattern of samples *10–12*

Table 4. Specific surface area data for samples *7–12*

Sample	Composition	Specific surface area S, m²/g
7	$Eu_{1.5}Gd_{0.5}Zr_2O_7$	0.600 ± 0.024
8	$EuGdZr_2O_7$	0.744 ± 0.029
9	$Eu_{0.5}Gd_{1.5}Zr_2O_7$	0.634 ± 0.025
10	$Eu_{1.5}Gd_{0.5}Hf_2O_7$	0.684 ± 0.027
11	$EuGdHf_2O_7$	0.987 ± 0.039
12	$Eu_{0.5}Gd_{1.5}Hf_2O_7$	0.890 ± 0.035

The dependence of the parameter a on the ionic radius ratio $r(Ln^{3+})/r(Zr(Hf^{4+}))$ was plotted on the basis of the calculated parameters (Fig. 5). As in the case of samples *1–6*, in samples *7–12* there is an increase in the parameter a with increasing radius ratio in the compound, i.e., with decreasing gadolinium content in the sample.

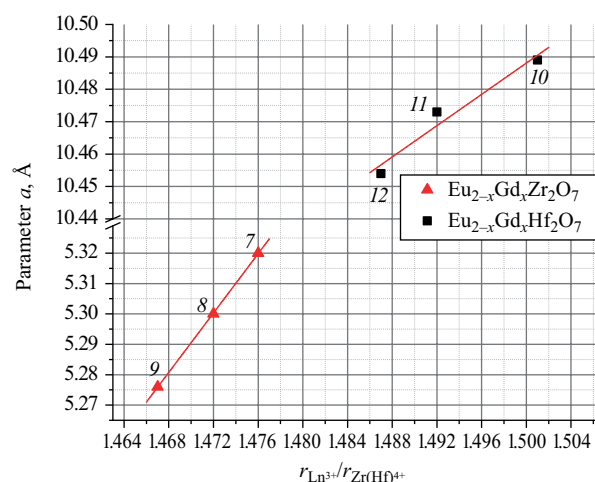The specific surface area of samples *7–12* was estimated by the BET method (Table 4).

The highest value of the specific surface area in each of the rows of samples is observed for the sample corresponding to the composition $EuGd(Zr/Hf)_2O_7$. In general, the specific surface area of the obtained powders does not exceed 1 m²/g. In [10], the specific surface area of gadolinium zirconate powder obtained by co-deposition method was 0.3 m²/g.
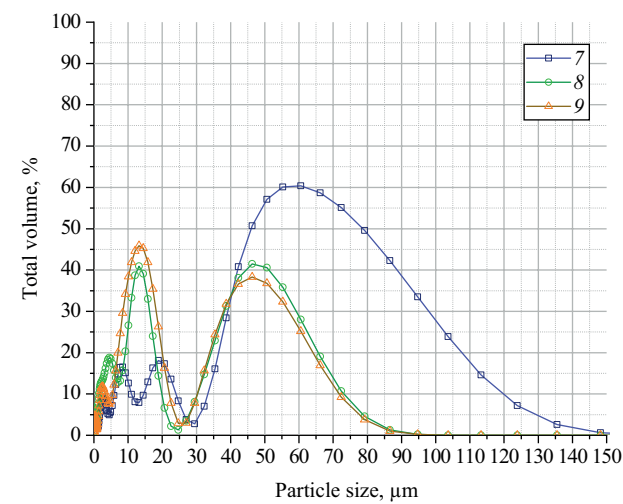
Fig. 6. Particle size distribution of samples *7* (marker •),
8 (marker ■), *9* (marker ▲)

Fig. 7. Particle size distribution of samples *10* (marker •),
11 (marker ■), *12* (marker ▲)

The particle size distribution was investigated by laser diffraction method. The particle size distribution curves for samples *8* and *9* (Fig. 6) show the presence of two intense peaks, indicating that the samples predominantly contain particles having sizes between 15 ± 10 and 45 ± 15 μm. The curve characterizing sample *7* shows that most of the volume is occupied by particles with sizes between 45 ± 10 and 90 ± 15 μm. Particles >100 μm occupy no more than 20%, while for samples *8* and *9* there are no particles of this fraction (Fig. 6).

The particle size distribution for samples *10–12* (Fig. 7) has a different character from that presented above. The Eu$_{2-x}$Gd$_x$Hf$_2$O$_7$ system predominantly contains particles having a size of 45 ± 15 μm for sample *12* and 60 ± 20 μm for sample *10*. Sample *11* has one broad peak with a maximum of about 70 μm, which covers almost the entire measurement range. For sample *12*, although the particle size does not exceed 100 μm, particles of this size account for about 20% of the sample and slightly more than 40% for sample *11*.

From a comparison of the two lines of samples, it can be concluded that samples *7–9* have a close to bimodal distribution of particles, while samples *10–12* tend rather to have one not highly intense but broad peak (monomodal distribution).

In order to investigate the CTEs, bulk ceramic samples were prepared. Measurements of the dimensional change of the samples were carried out in the temperature range of 300–1473 K. On the basis of the obtained data, the dependence of the ratio of the linear size difference to the initial size of the sample on the heating temperature was plotted (Fig. 8).
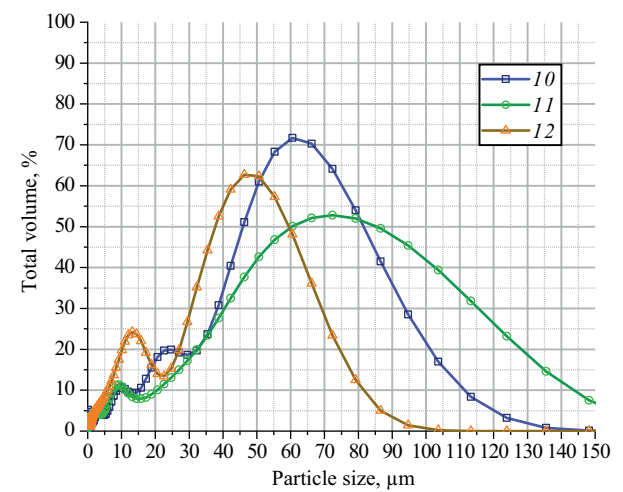
As can be seen from the presented dependencies, the difference in the behavior of samples *7–9* can be observed more clearly at temperatures above 700 K (Fig. 8), while the different behavior of samples *10–12* is more evident at temperatures above 600 K (Fig. 9).

The curves characterizing the dimensional change of samples *10–12* during heating (Fig. 9) have a linear character, which is practically useful for predicting the behavior of materials during utilization. Furthermore, the absence of jump-like changes in dimensions indicates the absence of phase transformations, i.e., the phase stability of samples at the main operating temperatures of materials based on them.

Using the obtained data, we calculated the CTEs of samples *7–12* (Table 5).

Table 5. CTE, $\alpha \cdot 10^{-6} \cdot \text{K}^{-1}$, of samples *7–12*

Sample	Composition	CTE, $\alpha \cdot 10^{-6} \cdot \text{K}^{-1}$
7	Eu$_{1.5}$Gd$_{0.5}$Zr$_2$O$_7$	9.17
8	EuGdZr$_2$O$_7$	9.02
9	Eu$_{0.5}$Gd$_{1.5}$Zr$_2$O$_7$	8.94
10	Eu$_{1.5}$Gd$_{0.5}$Hf$_2$O$_7$	9.83
11	EuGdHf$_2$O$_7$	9.81
12	Eu$_{0.5}$Gd$_{1.5}$Hf$_2$O$_7$	9.72

Figure 10 shows the dependence of CTE α on the ionic radius ratio $r(\text{Ln}^{3+})/r(\text{Zr}(\text{Hf}^{4+}))$.
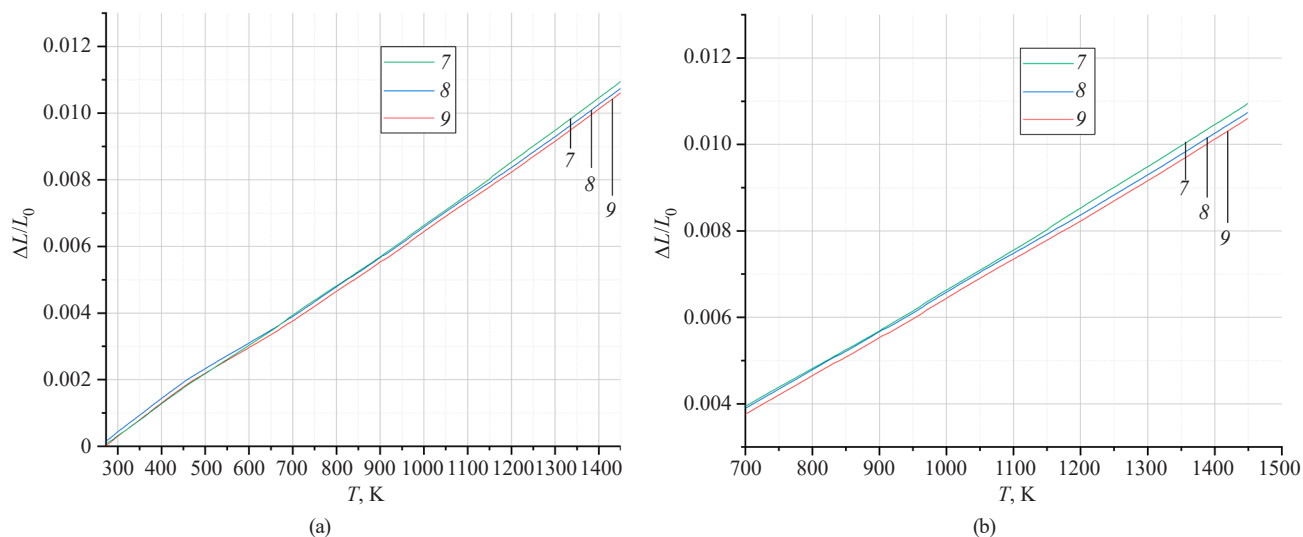
Fig. 8. Dependence of the ratio of the difference in sizes L to the initial size L_0 of the sample on the heating temperature T for samples *7–9* in the temperature range of 300–1473 K (a) and 700–1473 K (b)
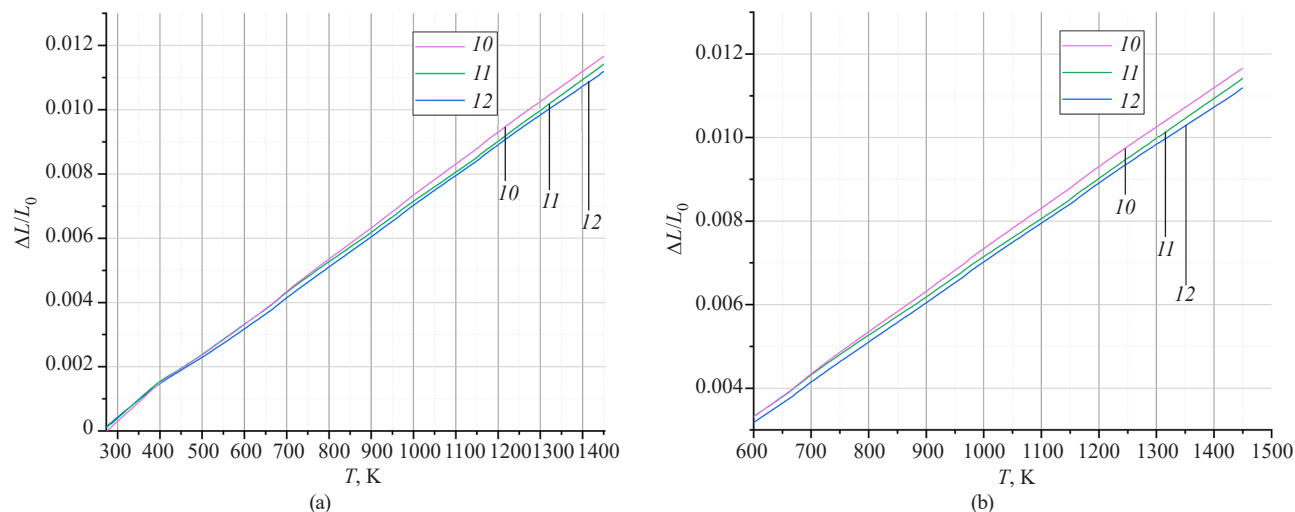

Fig. 9. Dependence of the ratio of the difference in sizes L to the initial size L_0 of the sample on the heating temperature T for samples *10–12* in the temperature range of 300–1473 K (a) and 600–1473 K (b)
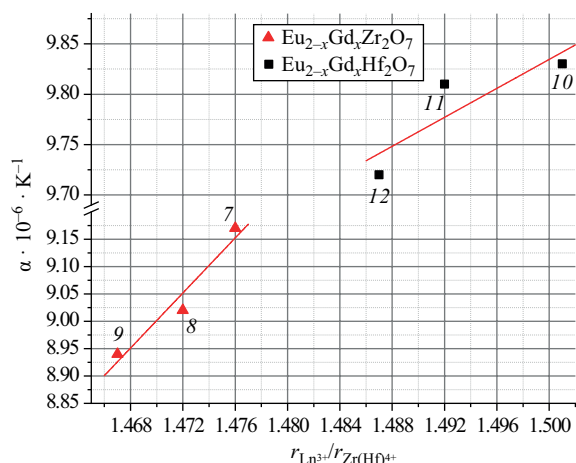

Fig. 10. CTE of samples *7–9* (markers ▲) and *10–12* (markers ■)

The presented graphs show an increase in CTE when the ratio of ionic radii in the samples increases, i.e., when the gadolinium content decreases (Fig. 10). This is due to the decreased parameter a of the unit cell fact that in samples with higher gadolinium content (and consequently decreased volume); as a consequence, the amplitude of its oscillation during heating decreases [28]. The difference of coefficients for different rulers of samples is also related to this: for samples *7–9* the average value of the unit cell parameter a is equal to ~5.3 Å (the fluorite structure is formed), while for samples *10–12* the average value of the unit cell parameter a is equal to ~10.5 Å (the value characteristic of the pyrochlore structure), which accounts for the different volume of the unit cell.

Since complex zirconates and hafnates have yet to be studied, the obtained CTE data can be compared with the literature data only for individual zirconates and hafnates of europium and gadolinium. Thus, in [29] CTE values are given for europium zirconate (Eu$_2$Zr$_2$O$_7$) of $10 \cdot 10^{-6}$ K^{-1} at 500 K, which increases to values of $11 \cdot 10^{-6}$ K^{-1} at 1500 K, as well as for gadolinium zirconate (Gd$_2$Zr$_2$O$_7$), which has the same values. In [30], the authors present the CTE curve for ceramic samples based on gadolinium zirconate, which has a parabolic character, where the CTE was $9 \cdot 10^{-6}$ K^{-1} at 673 K and $10.5 \cdot 10^{-6}$ K^{-1} at 1473 K temperature. For europium hafnate (Eu$_2$Hf$_2$O$_7$), the average value of CTE in the temperature range of 400–1200 K was $9.75 \cdot 10^{-6}$ K^{-1} [31], while the corresponding value for gadolinium hafnate (Gd$_2$Hf$_2$O$_7$) at 673 K of $\sim 12 \cdot 10^{-6}$ K^{-1} decreased to $11.3 \cdot 10^{-6}$ K^{-1} at 1473 K [32].

CONCLUSIONS

By contacting zirconium and hafnium hydroxides with europium and gadolinium acetates, single-phase REE zirconates and hafnates of the composition Eu$_{2-x}$Gd$_x$Zr$_2$O$_7$ and Eu$_{2-x}$Gd$_x$Hf$_2$O$_7$ were obtained under microwave heating conditions at $x = 0.5, 1.0, 1.5$. X-ray phase analysis confirmed the presence of fluorite structure in all samples following thermal treatment at 1473 K. Heat treatment at 1773 K leads to the formation of complex europium-gadolinium hafnates Eu$_{2-x}$Gd$_x$Hf$_2$O$_7$ having a pyrochlore structure. The unit cell and volume parameters were calculated for all phases. The results demonstrate that the increased gadolinium content in the synthesized phases leads to a linear decrease in the unit cell parameter a and consequent decrease in its volume. At the same time, the specific surface of the obtained powders does not exceed 1 m^2/g. The results of CTE measurements demonstrated that the dependence of the ratio of the size difference to the initial size of the sample on the heating temperature, along with the linear decrease in CTE with increasing gadolinium content in the samples, has a linear character.

Authors' contributions

N.V. Grechishnikov—conducting experimental studies, preparing the manuscript text, preparing materials for publication.

E.E. Nikishina—editing the manuscript text, preparing materials for publication, general supervision of the work.

The authors declare no conflict of interest.

REFERENCES

1. Lashmi P.G., Ananthapadmanabhan P.V., Unnikrishnan G., Aruna S.T. Present status and future prospects of plasma sprayed multilayered thermal barrier coating systems. *Eur. Ceram. Soc.* 2020;40(8):2731–45. https://doi.org/10.1016/j.jeurceramsoc.2020.03.016

2. Stanek C.R., Jiang C., Uberuaga B.P., Sickafus K.E., Cleave A.R., Grimes R.W. Predicted structure and stability of $A_4B_3O_{12}$ δ-phase compositions. *Phys. Rev. B.* 2019;80(17):174101. https://doi.org/10.1103/PhysRevB.80.174101

3. Sankar J., Kumar S. Synthesis of Rare Earth Based Pyrochlore Structured (A$_2$B$_2$O$_7$) Materials for Thermal Barrier Coatings (TBCs)-A Review. *Curr. Appl. Sci. Technol.* 2021;21(3):601–617. https://doi.org/10.14456/cast.2021.47

4. Salazar-Zertuche M., Díaz-Guillén J.A., Acosta-García J.O., Díaz-Guillén J.C., Montemayor S.M., Burciaga-Díaz O., Bazaldua-Medellin M.E., Fuentes A.F. Ionic conductivity of Ln$_4$Zr$_3$O$_{12}$ solid electrolytes synthesized by mechanochemistry. *Int. J. Hydrogen Energy.* 2019;44(24):12500–12507. https://doi.org/10.1016/j.ijhydene.2018.11.141

5. Popov V.V., Menushenkov A.P., Yaroslavtsev A.A., Zubavichus Y.V., Gaynanov B.R., Yastrebtsev A.A., Leshchev D.S, Chernikovet R.V. Fluorite-pyrochlore phase transition in nanostructured Ln$_2$Hf$_2$O$_7$ (Ln = La–Lu). *J. Alloys Compd.* 2016;689:669–679. https://doi.org/10.1016/j.jallcom.2016.08.019

6. Popov V.V., Menushenkov A.P., Zubavichus Y.V., *et al.* Studying processes of crystallization and cation ordering in Eu$_2$Hf$_2$O$_7$. *Russ. J. Inorg. Chem.* 2015;60(5):602–609. https://doi.org/10.1134/S0036023615050162
[Original Russian Text: Popov V.V., Menushenkov A.P., Zubavichus Y.V., Yaroslavtsev A.A., Veligzhanin A.A., Kolyshkin N.A., Kulik E.S. Studying processes of crystallization and cation ordering in Eu$_2$Hf$_2$O$_7$. *Zhurnal neorganicheskoi khimii.* 2015;60(5):672–680 (in Russ.). https://doi.org/10.7868/S0044457X15050165]

7. Popov V.V., Zubavichus Y.V., Menushenkov A.P., *et al.* Short- and long-range order balance in nanocrystalline Gd$_2$Zr$_2$O$_7$ powders with a fluorite-pyrochlore structure. *Russ. J. Inorg. Chem.* 2014;59(4):279–285. https://doi.org/10.1134/S0036023614040147

[Original Russian Text: Popov V.V., Zubavichus Y.V., Menushenkov A.P., Yaroslavtsev A.A., Kulik E.S., Petrunin V.F., Timofeeva N.N. Short- and long-range order balance in nanocrystalline Gd₂Zr₂O₇ powders with a fluorite-pyrochlore structure. *Zhurnal neorganicheskoi khimii*. 2014;59(4):431–438 (in Russ.).]

8. Sadykov V., Shlyakhtina A., Lyskov N., Sadovskaya E., Cherepanova S., Eremeev N., Skazka V., Goncharov V., Kharitonova E. Oxygen diffusion in Mg-doped Sm and Gd zirconates with pyrochlore structure. *Ionics* (*Kiel*). 2020;26(9):4621–4633. https://doi.org/10.1007/s11581-020-03614-5

9. Chernov I.O., Kushtym A.V., Malykhin S.V,. Synthesis of Materials Based on Compounds of Rare Earth Elements With Titanium, Hafnium and Zirconium As Promising Neutron Absorbers for Nuclear Reactors. *Probl. Atomic Sci. Technol.* 2024;2024(4):64–78. http://doi.org/10.46813/2024-152-064

10. Torres-Rodriguez J., Gutierrez-Cano V., Menelaou M., Kaštyl J., Cihlář J., Tkachenko S., Gonzalez J., Kalmar J., Fabian I., Lazar I., Celko L., Kaiser J. Rare-Earth Zirconate Ln₂Zr₂O₇ (Ln: La, Nd, Gd, and Dy) Powders, Xerogels, and Aerogels: Preparation, Structure, and Properties. *Inorg. Chem.* 2019;58(21):14467–14477. https://doi.org/10.1021/acs.inorgchem.9b01965

11. Zhang A., Lü M., Yang Z., Zhou G., Zhou Y. Systematic research on RE₂Zr₂O₇ (RE = La, Nd, Eu and Y) nanocrystals: Preparation, structure and photoluminescence characterization. *Solid State Sci.* 2008;10(1):74–81. https://doi.org/10.1016/j.solidstatesciences.2007.07.037

12. Matovic B., Maletaskic J., Zagorac J., Pavkov V., Maki R., Yoshida K., Yano T. Synthesis and characterization of pyrochlore lanthanide (Pr, Sm) zirconate ceramics. *J. Eur. Ceram. Soc.* 2020;40(7):2652–2657. https://doi.org/10.1016/j.jeurceramsoc.2019.11.012

13. Zeng J., Wang H., Zhang Y.C., Zhu M.K., Yan H. Hydrothermal synthesis and photocatalytic properties of pyrochlore La₂Sn₂O₇ nanocubes. *J. Phys. Chem. C.* 2007;111(32):11879–11887. https://doi.org/10.1021/jp0684628

14. Wang Q., Cheng X., Li J., Jin H. Hydrothermal synthesis and photocatalytic properties of pyrochlore Sm₂Zr₂O₇ nanoparticles. *J. Photochem. Photobiol. A: Chemistry.* 2016;321:48–54. https://doi.org/10.1016/j.jphotochem.2016.01.011

15. Perera S.S., Munasinghe H.N., Yatooma E.N., Rabuffetti F.A. Microwave-assisted solid-state synthesis of NaRE(MO₄)₂ phosphors (RE = La, Pr, Eu, Dy; M = Mo, W). *Dalton Trans.* 2020;49(23):7914–7919. https://doi.org/10.1039/D0DT00999G

16. Fetter G., Bosch P., Lopez T. ZrO₂ and Cu/ZrO₂ Sol–Gel Synthesis in Presence of Microwave Irradiation. *J. Sol- Gel Sci. Technol.* 2002;23:199–203. https://doi.org/10.1023/A:1013983211564

17. Vanetsev A.S., Tretyakov Y.D. Microwave-assisted synthesis of individual and multicomponent oxides. *Russ. Chem. Rev.* 2007;76(5):397–413. https://doi.org/10.1070/RC2007v076n05ABEH003650
[Original Russian Text: Vanetsev A.S., Tretyakov Y.D. Microwave-assisted synthesis of individual and multicomponent oxides. *Uspekhi khimii.* 2007;76(5):435–453 (in Russ.). https://doi.org/10.1070/RC2007v076n05ABEH003650]

18. Długosz O., Szostak K., Banach M. Photocatalytic properties of zirconium oxide–zinc oxide nanoparticles synthesised using microwave irradiation. *Appl. Nanosci.* 2020;10(3):941–954. https://doi.org/10.1007/s13204-019-01158-3

19. Kucio K., Sydorchuk V., Khalameida S., Charmas B. Mechanochemical and microwave treatment of precipitated zirconium dioxide and study of its physical–chemical, thermal and photocatalytic properties. *J. Therm. Anal. Calorim.* 2022;147:253–262. https://doi.org/10.1007/s10973-020-10285-x

20. Batool T., Bukhari B.S., Riaz S., Batoo K.M., Raslan E.H., Hadi M. Microwave assisted sol–gel synthesis of bioactive zirconia nanoparticles–correlation of strength and structure. *J. Mech. Behav. Biomed. Mater.* 2020;112:104012. https://doi.org/10.1016/j.jmbbm.2020.104012

21. Mahendran N., Johnson Jeyakumar S., Jothibas M., Ponnar M., Muthuvel A. Synthesis, characterization of undoped and copper-doped hafnium oxide nanoparticles by sol–gel method. *J. Mater. Sci.: Mater. Electron.* 2022;33(13):10439–10449. https://doi.org/10.1007/s10854-022-08031-0

22. Grechishnikov N.V., Nikishina E.E., Il'icheva A.A., Podzorova L.I. Effect of microwave treatment on the phase composition of europium zirconate during dilution synthesis. *Tsvetnye Metally.* 2023;10:51–55 (in Russ.). https://doi.org/10.17580/tsm.2023.10.06

23. Fuentes A.F., O'Quinn E.C., Montemayor S.M., Zhou H., Lang M., Ewing R.C.. Pyrochlore-type lanthanide titanates and zirconates: Synthesis, structural peculiarities, and properties. *Appl. Phys. Rev.* 2024;11(2):021337. https://doi.org/10.1063/5.0192415

24. Talanov M.V., Talanov V.M. Formation of breathing pyrochlore lattices: Structural, thermodynamic and crystal chemical aspects. *CrystEngComm.* 2020;22(7):1176–1187. https://doi.org/10.1039/C9CE01635J

25. Shannon R.D. Revised effective ionic radii and systematic studies of interatomic distances in halides and chalcogenides. *Acta Cryst. Sect. A.* 1976;32(5):751–767. https://doi.org/10.1107/S0567739476001551

26. Saradhi M.P., Ushakov S.V., Navrotsky A. Fluorite-pyrochlore transformation in Eu₂Zr₂O₇ – Direct calorimetric measurement of phase transition, formation and surface enthalpies. *RSC Adv.* 2012;2(8):3328–3334. https://doi.org/10.1039/c2ra00727d

27. Pavlyuchkov D., Seidel J., Dzuban A., Savinykh G., Schreiber G. Heat capacity for the Eu₂Zr₂O₇ and phase relations in the ZrO₂–Eu₂O₃ system: Experimental studies and calculations. *Thermochim. Acta.* 2013;558:74–82. https://doi.org/10.1016/j.tca.2013.02.009

28. Liu X., Wang H., Wang W., Fu Z.. A prediction model of thermal expansion coefficient for cubic inorganic crystals by the bond valence model. *J. Solid. State. Chem.* 2021;299:122111. https://doi.org/10.1016/j.jssc.2021.122111

29. Kutty K.V., Rajagopalan S., Mathews C.K., Varadaraju U.V. Thermal expansion behaviour of some rare earth oxide pyrochlores. *Mater. Res. Bull.* 1994;29(7):759–66. https://doi.org/10.1016/0025-5408(94)90201-1

30. Liu Z, Shen Z, Liu G, He L, Mu R, Xu Z. Sm-doped Gd₂Zr₂O₇ thermal barrier coatings: Thermal expansion coefficient, structure and failure. *Vacuum.* 2021;190:110314. https://doi.org/10.1016/j.vacuum.2021.110314

31. Hagiwara T., Nomura K., Kageyama H. Crystal structure analysis of Ln₂Zr₂O₇ (Ln = Eu and La) with a pyrochlore composition by high-Temperature powder X-ray diffraction. *J. Ceram. Soc. Japan.* 2017;125(2):65–70. https://doi.org/10.2109/jcersj2.16248

32. Yang P., An Y., Yang D., Li Y., Chen J. Structure, thermal properties and hot corrosion behaviors of Gd₂Hf₂O₇ as a potential thermal barrier coating material. *Ceram. Int.* 2020;46(13):21367–21377. https://doi.org/10.1016/j.ceramint.2020.05.234

About the Authors

Nikolay V. Grechishnikov, Postgraduate Student, K.A. Bol'shakov Department of Chemistry and Technology Rare Elements, M.V. Lomonosov Institute of Fine Chemical Technologies, MIREA – Russian Technological University (78, Vernadskogo pr., Moscow, 119454, Russia). E-mail: nklgrchshnkv@yandex.ru. Scopus Author ID 58683791100, https://orcid.org/0009-0003-9591-391X

Elena E. Nikishina, Cand. Sci. (Chem.), Associate Professor, K.A. Bol'shakov Department of Chemistry and Technology Rare Elements, M.V. Lomonosov Institute of Fine Chemical Technologies, MIREA – Russian Technological University (78, Vernadskogo pr., Moscow, 119454, Russia). E-mail: nikishina@mirea.ru. Scopus Author ID 6602839662, ResearherID O-7115-2014, RSCI SPIN-code 9403-2325, https://orcid.org/0000-0003-3579-2194

Об авторах

Гречишников Николай Владимирович, аспирант, кафедра химии и технологии редких элементов им. К.А. Большакова, Институт тонких химических технологий им. М.В. Ломоносова, ФГБОУ ВО «МИРЭА – Российский технологический университет» (119454, Россия, Москва, пр-т Вернадского, д. 78). E-mail: nklgrchshnkv@yandex.ru. Scopus Author ID 58683791100, https://orcid.org/0009-0003-9591-391X

Никишина Елена Евгеньевна, к.х.н., доцент, кафедра химии и технологии редких элементов им. К.А. Большакова, Институт тонких химических технологий им. М.В. Ломоносова, ФГБОУ ВО «МИРЭА – Российский технологический университет» (119454, Россия, Москва, пр-т Вернадского, д. 78). E-mail: nikishina@mirea.ru. Scopus Author ID 6602839662, ResearherID O-7115-2014, SPIN-код РИНЦ 9403-2325, https://orcid.org/0000-0003-3579-2194

Translated from Russian into English by H. Moshkov
Edited for English language and spelling by Thomas A. Beavitt